













Coastal wetland responses to a century of climate change in northern Sahara, Morocco

Juliana Nogueira ^{1,2,3*} Heitor Evangelista ^{1,3} Lhoussaine Bouchaou ^{4,5} Luciane Moreira ³
Abdelfettah Sifeddine ⁶ Ahmed ElMouden,⁴ Fouad Msanda,⁴ Sandrine Caquineau ⁶
Francisco Javier Briceño-Zuluaga ⁷ Marcus Vinicius Licínio ⁸ Magloire Mandeng-Yogo,⁶
Mercedes Mendez-Millan ⁶ Renato C. Cordeiro ³ Bastiaan Knoppers ³ Manuel Moreira-Ramírez ³
Renato Martins¹

¹LARAMG – Radioecology and Climate Change Laboratory, Department of Biophysics and Biometry, Rio de Janeiro State University, Rua São Francisco Xavier, Rio de Janeiro, Rio de Janeiro, Brazil

²Faculty of Forestry and Wood Sciences, Czech University of Life Sciences Prague, Prague, Czech Republic

³Postgraduate Program in Geochemistry, Department of Geochemistry, Institute of Chemistry, Fluminense Federal University, Niterói, Rio de Janeiro, Brazil

⁴Laboratory of Applied Geology and Geo-Environment, Ibn Zohr University, Agadir, Morocco

⁵International Water Research Institute (IWRI), Mohammed VI Polytechnic University (UM6P), Ben Guerir, Morocco

⁶IRD, Sorbonne Université, CNRS, MNHN, IPSL, LOCEAN, Bondy, France

⁷Facultad de Ciencias Básicas - Universidad Militar Nueva Granada, Bogotá, Colombia

⁸Department of Physiological Sciences, CCS - UFES, Environmental Radiometry Laboratory - CCS - Federal University of Espírito Santo – UFES, Vitória, Espírito Santo, Brazil

Abstract

Coastal wetlands are highly sensitive to changes occurring at the coastline. It is critically important to determine region-specific projections for these areas due to their specificities and vulnerabilities to climate change. This work aimed to value the impacts of recent climate changes at West Africa Sahara coastland, southern Morocco, at Khnifiss Lagoon. We have applied a combined approach using remote sensing techniques and environmental reconstructions based on high-resolution analysis of sediment cores, covering the current warm period. Remote sensing highlighted changes to the lagoon inlet, accompanied by a greater meandering character of the tidal channels. As a response, the sediment cores have recorded a predominant vegetation substitution due to changes in the tidal limit, and an increase in organic carbon accumulation was observed. For the current climatology, during positive phases of the North Atlantic Oscillation, winds reaching the coast strengthen in an east-to-west direction. In the Khnifiss Lagoon, whose inlet is dominated by the ebb tide, the intensity and direction of the winds on the coast at surface level modifies its connection to the ocean by increasing sediment transport toward the interior of the lagoon. Locally biological responses to wind intensification, and possibly sea-level rise, exemplify the lagoon sensitivity to large-scale processes. Coastal vegetated wetlands are considered to be highly dynamic environments. However, we expect a loss of the upper tidal vegetation due to boundary conditions limiting the accommodation space in this arid environment in a possible future scenario of continuously inland tidal line displacement.

*Correspondence: junogueira@id.uff.br

This is an open access article under the terms of the Creative Commons Attribution-NonCommercial-NoDerivs License, which permits use and distribution in any medium, provided the original work is properly cited, the use is non-commercial and no modifications or adaptations are made.

Additional Supporting Information may be found in the online version of this article.

Deputy editor: Julia C. Mullarney

[Correction added on 04 February 2022, after first online publication: Affiliation has been changed from 2 to 3 for the following authors: Heitor Evangelista, Luciane Moreira, Renato C. Cordeiro, Bastiaan Knoppers and Manuel Moreira-Ramírez]

The most important transition environments between terrestrial and marine ecosystems are coastal vegetated wetlands such as salt or fresh marshes, mudflats, mangrove swamps, and submerged seagrass (Viaroli et al. 2007). These zones are located close to the coastal line in estuarine or lagoon systems and undergo tidal influence, characterized by permanent or periodical salt or brackish water influx (Rey 2016). Complex interactions among stressors and autochthonous and allochthonous material fluxes from land, ocean, and atmosphere control the ecosystem evolution, resulting in a highly dynamic and vulnerable environment (Viaroli et al. 2007). Factors such as sea-level rise, heavy precipitation runoff during storms, and anthropogenic action are among

the most considerable impacts on coastal wetlands (Crossland et al. 2005). These factors can cause changes in wetland extent and morphology (Schuerch et al. 2018) and, indirectly, consequences for its biota and biological interactions (Day et al. 2008).

Mangroves and saltmarshes contribute between 2000 and 215,00 US\$ ha⁻¹ yr⁻¹ (Macreadie 2020) to coastal economies through the delivery of ecosystem services such as nature-based flood and erosion protection (Möller et al. 2014), “blue carbon” burial (Macreadie 2020; Richir et al. 2020), support to fishing activities (Aburto-Oropeza et al. 2008), tourism, and as barrier to coastal pollutants and pathogens (Richir et al. 2020). Above all, they also provide habitat to various species, including commercially important fisheries stocks and threatened birds and mammals (Richir et al. 2020).

Many societies depend on coastal productivity, which can sum up to 15% of the animal protein and support 10–12% of the global population (Barua et al. 2020). The fishery is vital for the economy of developing countries, which, together, contribute to 54% of global fishery exportation (FAO 2018), and where most of the people who depend on this activity—and who also deal with low incoming and limited food resources—live. In arid areas, where resources are naturally scarce, coastal wetlands play a significant role in the sustenance of local population and biota—which may include endemic species.

Multi-time-scale natural archives indicate that coastal wetlands are sensitive to changes occurring at the coastline (McFadden et al. 2007). It is critically important to determine region-specific expected future changes once wetlands are diverse environments with specificities and different vulnerabilities to climate change (Day et al. 2008; Erwin 2009).

Morocco has a coastal zone of 3500 km, in the Atlantic Ocean and in the Mediterranean Sea, comprising a maritime area of about 1.2 million km². Its fishing potential is estimated to be 1.5 million tons, renewable each year, as inferred by the FAO (Food and Agriculture Organization of the United Nations) (Royaume du Maroc 2015). The fishing sector in Morocco is the third most important national economy, below agriculture and tourism. The Khnifiss Lagoon is the only example of a continental-marine environment in the Moroccan Sahara (Dakki and de Ligny 1988). Away from any high human impact activities, it is classified as a Site of Biological and Ecological Interest of great natural and sociocultural importance (AEFCS 1996). This Ramsar site provides resources for the local population—in terms of the fishery, grazing, and tourism—and for the local biodiversity, including endemic species and a significant amount of intercontinental migratory birds.

Our objective is to comprehend better the regional impacts of climate change on coastal ecosystems in North Africa during the recent past. Understanding the relationship between the modes of climate variability known in the literature as much as the response and tendencies of these rare coastal environments is crucial for predicting possible impacts and planning adaptation and mitigation strategies.

Because instrumental records are limited to the last few decades for the West Africa Sahara coastland, we have applied a combined approach using both remote sensing data and reconstructed past environments from biogeochemical and physical proxies recovered from high-resolution sediment cores layers—to evaluate better the recent change (since ~ 1901) on Khnifiss Lagoon ecosystem.

Methods

The Khnifiss Lagoon

The Khnifiss Lagoon (28°02'54"N, 12°13'66"W), 20 km long and 65 km² of surface area, is located on the southern Atlantic coast of Morocco, 170 km from the city of Laâyoune (Fig. 1a), in an upwelling region of great importance, Cape Ghir (McGregor et al. 2007). The lagoon is characterized by a small and shallow basin with rare freshwater contribution from the temporary river (Oued) Aouedri and a perennial connection with the Atlantic Ocean, the inlet Fom Agoutir (Dakki and de Ligny 1988). It presents a configuration of a tidal creek, characterized by shallow channels of muddy bottom, subject to the tide action. The Khnifiss Lagoon tidal dynamic is characterized by two cycles of bidirectional and alternating currents with a duration of approximately 24 h. For each cycle, two phases are observed equivalent to the filling and the emptying of the lagoon. The tidal range varies between around 1.5–2 m, thus being characterized as a microtidal environment. A tidal lag is observed, with an increase related to the distance into the lagoon (El Agbani et al. 1988).

The local geomorphology comprises dendritic channels that fill with the tide and taper toward the upstream. The intertidal flats, also called mudflats, generally surround the tidal creek and are located at the high tide limit (or above). Seawater is confined to the main channel, except during spring tides. The tidal channels are interconnected and flanked by extensive salt marshes, exhibiting a variety of vegetation, most of them halophytes (Fig. 1b–d), previously described for the site (Hammada 2007). Within the tidal community, it is usually possible to identify a clear zoning pattern, typically linked to resistance and adaptation to flood and salinity, as depicted in Fig. 1b for the case of the Khnifiss Lagoon. The saltmarsh is vegetated by halophytic herbs, grasses (pioneers), and low shrubs at the lower and upper marsh adapted to regular or occasional submergence by the tides, respectively.

The Khnifiss Lagoon presents a real complex of habitats: the intertidal channels; intertidal areas and mudflats; areas covered by *Zostera* or algae in shallow zones; plains between the channels, dominated by *Spartina*; extensive salicornes; and the Tazra and Mzeira salt flats (sebkhas). Data from the Ramsar sheet indicate that the Khnifiss Park, which includes the lagoons and surrounding areas, is home to several vulnerable or threatened species at a national or international level.

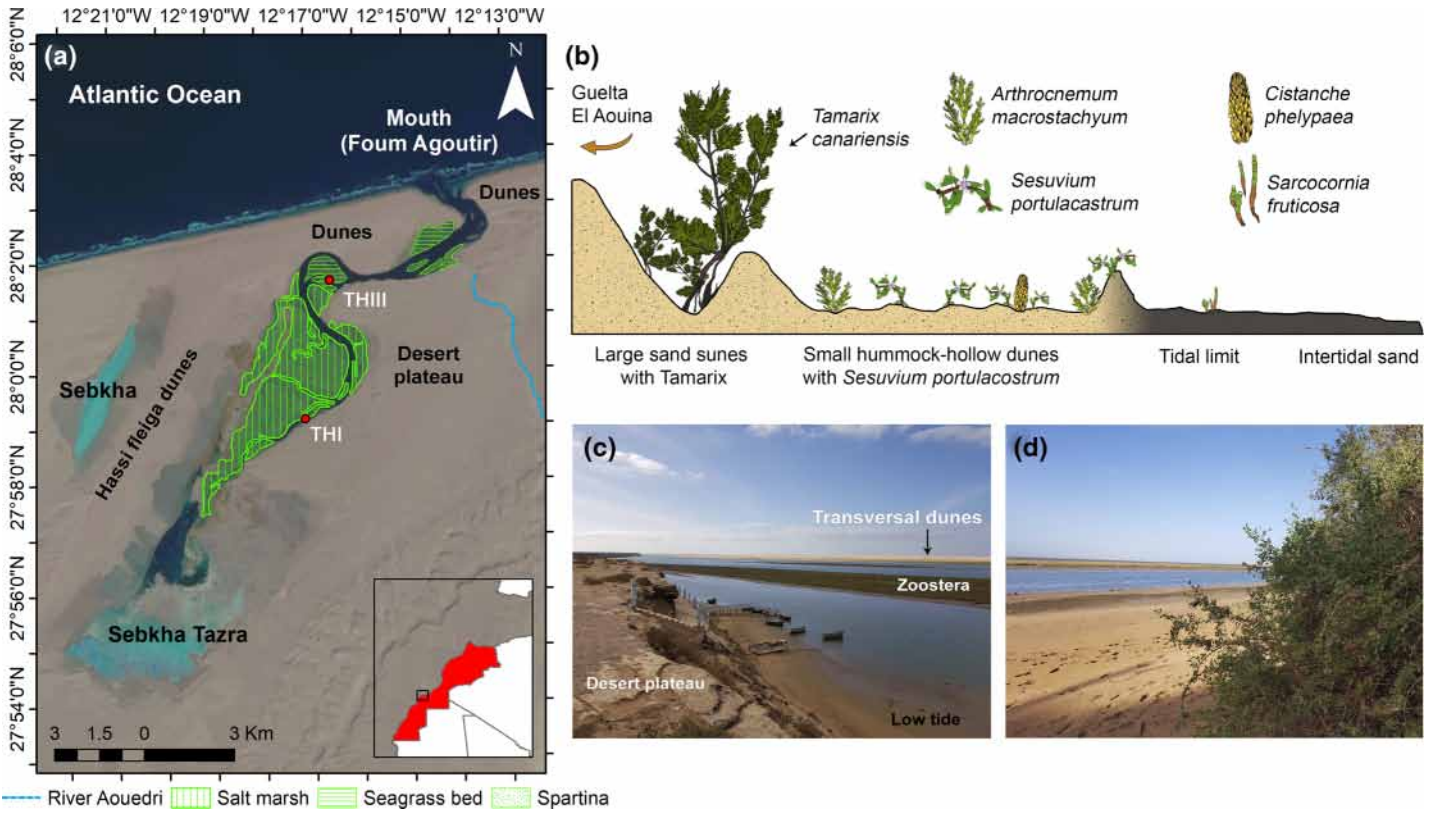


Fig. 1. (a) The Khnifiss Lagoon (southern Morocco) surroundings exhibit a combination of salt flats (sebkhas), dunes, and saltmarsh vegetation (in green). The red dots are the recovering points for THIII and THI sediment cores; (b) vegetation distribution profile around the waterbody; (c and d) pictures of the studied area during low tide.

Remote sensing

According to availability and cloud coverage, satellite images were chosen for each decade, representing the wet (November to March) and dry period (April to October) between 1972 and 2016, totaling 23 images previously radiometrically corrected. The images, whose information is described in Table S1, were obtained from the Earth Explorer USGS database, accessed at <http://earthexplorer.usgs.gov>, courtesy of the U.S. Geological Survey.

We have explored the vegetation coverage around the lagoon based on its spectral signature. Vegetation exhibits high absorption in the visible region and high reflectance in the near-infrared properties used in remote sensing to define reflectance indices. Herein, we have used the Soil Adjusted Vegetation Index (SAVI) (Huete 1988), which takes into account the normalization of soil color and exposure variations, setting the constant parameter “L” and therefore highlighting the vegetation cover. The parameter “L” varies from 0 (areas with very dense vegetation cover) to 1 (areas with little vegetation cover). For the Khnifiss Lagoon surroundings, a value of 0.5 was applied since medium cover was observed. We have used the maximum SAVI values as an additional parameter to understand the vegetation vitality tendencies and compare them with other remote sensing-derived

data. Beyond vegetation area coverage and vitality, the SAVI values were used as a tool for satellite image classification. Pixels in the images were identified as water, sandy terrain, salt flat, intertidal terrain, or vegetation by applying an object-oriented image classification (Congalton and Green 2019). Once a pixel in a satellite image represents a known area defined by the spatial resolution, specific for each satellite sensor and ranging from 30 to 80 m (Table S1), it is possible to obtain each feature coverage area based on the number of pixels previously classified, through the years. Given the extensive coverage area of the features of interest, the spatial resolution is enough for their satisfactory classification. Also, as dealing with changes in a landscape level, the analysis of a few images representing the dry and wet periods—limited by images availability—is enough to observe tendencies in the features dynamics throughout the analyzed period.

As a result of erosion, the meander of a channel becomes more curved proportionally to the speed and volume of water entering the system (Julien 2018). The distance between the lagoon inlet and the apparent end of the main channel was measured for each image, based on the classified pixels, to calculate the Meandering Index. For this index, values close to 1 represent highly rectilinear channels. In contrast, the increase in this value follows an increase in the meandering

character of the analyzed system (see Fig. S1 for details). We have also measured the inlet opening width through the years, using control points as a reference.

To investigate the impact of winds on the lagoon geomorphology, remote sensing derived data were used, according to datasets available variables. Wind speed data at 10 m derived from ERA-40 (Uppala et al. 2005) and ERA-Interim (Berrisford et al. 2011) were accessed through the ClimateReanalyzer.org portal of the Institute of Climate Change of the University of Maine (USA). ERA-40 ($1.125^\circ \times 1.125^\circ$ global grid) and ERA-Interim ($0.75^\circ \times 0.75^\circ$ global grid) data were used to understand the regional impact of the winds in the coast given their spatial resolution. We have also used sea surface winds data derived from the NOAA/NCDC blended daily global 0.25° Sea Surface Winds archive (Zhang et al. 2006) to understand the wind stress at the coast. Surface wind vector, derived from NCEP/NCAR Reanalysis ($2.5^\circ \times 2.5^\circ$ global grid) (Kalnay et al. 1996), was used to investigate the wind pattern relation with large-scale atmospheric dynamics, that is, comparing it with the North Atlantic Oscillation (NAO) phases time series (NOAA/ESRL PSL). Sea-level data from satellite altimeter estimations (Church and White 2011) and tide gauges measurements (Caldwell et al. 2015) were considered.

Sediment cores

Sediment cores recovery and bulk density estimation

The cores measuring approximately 50 cm were collected manually from a boat employing a gravity core sampler. The cores were sliced every 2 cm in the field, packed in individually identified plastic bags, and kept refrigerated. The THIII sediment core ($28^\circ 01.626'N$, $12^\circ 16.558'W$), measuring 48 cm in length, was recovered in one of the lagoon's main water entrance channel sections. This site is approximately 5–8.7 m deep (Idrissi et al. 2004) and lies between two islets of exposed sediment dominated by marine grass specimens of *Zostera noltii*. Due to its proximity to the inlet, this site is highly influenced by the seawater entrance and ocean nutrients. It presents a higher current velocity between $56\text{--}78\text{ cm s}^{-1}$ and bottom sediments composed of sandy clay. The THI sediment core ($27^\circ 59.139'N$, $12^\circ 17.109'W$), located in the inner portion of the lagoon, was retrieved from a secondary channel, having 52 cm in length. To its east side, the secondary channel is protected by a desert plateau. To its west lies a saltmarsh area, occupied by specimens of the genus *Salicornia* sp., periodically exposed by tidal dynamics. A low marine influence characterizes this part of the lagoon, depths between 2.70 and 5.20 m, during low and high tides, respectively (Idrissi et al. 2004), and surrounded by extensive heterogeneous marshes. The saltmarsh currently shelters plant species such as *Arthrocnemum macrostachyum*, *Atriplex portulacoïdes*, *Salicornia* sp., and *Zygophyllum gaetulum*, adapted to soils often submerged by the action of the tides. Salinity was measured for each sampling site using a YSI® 188 Professional Plus multiparameter sonde.

Bulk density measurements were realized through the mass-volume method and expressed as g cm^{-3} .

Sediment core dating and sedimentation rates estimation

The sedimentation rates and chronology of each sediment layer were determined by the Constant Initial Concentration model (Robbins and Edgington 1975) using natural radionuclides ^{210}Pb and ^{226}Ra and the 1965 bomb peak for ^{137}Cs . The sediment samples were dried in an oven at 50°C for 48 h, ground in an agate mortar, and stored in sealed disposable plastic Petri dishes. The samples were weighed and the densities were measured. The high-resolution gamma-ray measurements were performed for 24 h for each sample using a plane coaxial extended range germanium hyper pure detector (model GX5021), installed at the Department of Physiological Sciences of the Espírito Santo Federal University (UFES), Brazil. Detector relative efficiency is 50%, with a resolution of 2.1 KeV (FWHM) at the ^{60}Co peak (1.33 MeV).

Geochemical analysis

To determine the origin of the sedimentary organic matter, elemental and isotopic concentrations of carbon and elemental S and N were analyzed. The samples were lyophilized, macerated in an agate mortar, and weighed. An aliquot of each sample was analyzed at the elemental analyzer Vario El III Elementary (Elementar) for total carbon, nitrogen, and elemental sulfur concentrations with a precision of 0.05 for %C, 0.05 for %N, and 0.2% for sulfur. The remaining aliquot was used to determine $\delta^{13}\text{C}$ and organic carbon. Samples were subjected to acid attack (HCl 3%) until the carbonate fraction was removed. Elemental organic carbon and organic carbon isotopes were analyzed with a FlashHT 2000 elemental analyzer coupled with a Delta V Advantage mass spectrometer from Thermo Fisher Scientific with a precision of 0.05 permil for $\delta^{13}\text{C}$ and 0.05% for organic carbon. The $\delta^{13}\text{C}$ is expressed in per mil (‰) against the international standard VPDB (Vienna Pee Dee Belemnite).

Aiming at a better recognition of the carbon and nitrogen signature nature at the different layers in the sediment core and avoiding the use of generic ranges for these isotopes, the local vegetation specimens were collected and analyzed for their elemental and isotopic analysis of C and N. The methodology and further information are detailed in Supplementary Text 1 and Table S6.

Carbon flux for the Khnifiss Lagoon was calculated from both sediment cores, considering its sedimentation rates—when available, total organic carbon (TOC) content, and bulk density. Values were expressed in terms of $\text{g C m}^{-2}\text{ yr}^{-1}$.

Finally, Sr, Ca, Si, and Ti concentrations were determined using an Epsilon 3^X energy dispersive X-ray fluorescence (XRF) spectrometer, PANalytical. A total of 50 samples (26 and 24 for THI and THIII, respectively) were milled into powder and transferred to an open-ended XRF cup covered with a $3.6\ \mu\text{m}$ PANalytical thin film. The reference concentration for each element was based on the concentration of the element, using inter-element slope and baseline-corrected peak heights from the XRF system.

Granulometric analysis

The samples for particle size analysis were treated with 1 N HCl at 25°C to remove carbonates. Once the digestion process was completed, the samples were washed with distilled water and then were centrifuged at 4000 rpm, after which the supernatant was carefully removed using a Pasteur pipette. After this step, the samples had their organic matter content removed by treatment with concentrated hydrogen peroxide (30%) that was continually added to the sample in a hot plate at 60°C until sample frothing ceased. A dispersant (sodium hexametaphosphate [NaPO₃]₆, 40 mg L⁻¹) was added to avoid particle aggregation, which could interfere in the determination of the particle size distribution. Thus, only the mineral fraction of the sample remained, presenting no agglutination between the particles. The samples were shaken for 24 h and then analyzed in the CILAS® 1064 Particle Analyzer. The CILAS 1064 has a dual sequenced laser system for a measuring range of 0.04–500 μm and delivers the results in 100 interval classes.

Sedimentary chlorophyll derivatives

To determine chlorophyll derivatives in sediment, we applied the method described by Sanger and Gorham (1972). The “sedimentary chlorophyll,” a product of chlorophyll degradation, was extracted from sediments by placing approximately 1 g of wet sample to a centrifuge tube, protected from ambient light with laminated paper, and by adding 20 mL of 90% acetone in each tube. The tubes were left on a shaking table, in a semi-dark environment, for approximately 20 min for two consecutive times, interspersed by centrifugation and removal of the supernatant, and with a third extraction, adding 10 mL of acetone. The absorbance of the extract was measured in a scanning spectrophotometer with a range of 350–800 nm. The possible interferences in the absorbance background were corrected by subtracting the chlorophyll peaks from a baseline curve made between 500 and 800 nm, thus eliminating the absorbance of nonchlorophyll components (Wetzel 2001). The concentrations of pigments are expressed as the Sediment Pigment Derivative Unit (SPDU) per gram of organic matter (Vallentyne 1955).

To support the multiproxy interpretation and discussion, a principal component analysis (PCA) was performed for each core data using the Statistica software by StatSoft.

Results and discussion

Remote sensing

Applying the object-oriented classification, which used both spectral and spatial information from the 19 remote sensing images analyzed, it was possible to identify the distinct landscape features covering the areas over the last ~ 44 yr (Fig. S2). The area occupied by the waterbody presents an antiphase behavior over time compared to the vegetation extension. Once the waterbody increases in volume, the water

column covers the vegetation that once was exposed to the satellite’s sensor (Fig. S3; Table S2).

The Khnifiss Lagoon is a meandering system strongly influenced by the volume of water entering it from the Atlantic Ocean. Changes in the water entry regime to the lagoon—such as changes in the inlet or sea level—may have a more significant impact on the local ecology than other variables such as precipitation due to the insertion in a desertic environment. In this way, Fig. S4 depicts a comparison among the maximum registered SAVI values during both dry and wet seasons, the normalized inlet size, the Meandering Index, and the vegetation coverage area. A decreasing trend is observed for the SAVI values (Table S3), indicating decay in general vegetation vitality and coverage. In contrast, the inlet width (Table S4) and the meandering index (Table S5) exhibited an increasing behavior, indicating a possible higher water intake in response to a broader inlet. Therefore, we can infer that a process of the lagoon’s inlet opening led to a more meandric character of the ecosystem resulting in more vegetation area coverage by the water body.

Sediment cores

From the sediment cores’ geochemical and physical characteristics, we observed a progressive inflow of seawater into the lagoon since the early 1970s. This record is in concordance with our satellite data compilation.

Chronology of the sediment core THI spans 1928–2014, resulting in an 86-yr record of the Khnifiss Lagoon (Fig. S5). During the sampling, salinity at the site was 40 PSU (Practical Salinity Unit). The sedimentation rate (Fig. S5b) revealed a tendency of increase since the year 1975, indicating that the lagoon environment became increasingly prone to deposition. On the other hand, the TOC content (Fig. 2a) showed an opposite trend, probably reflecting a decrease of allochthonous vegetal biomass at the THI site. The chlorophyll derivatives, however, remained relatively stable (~ 12.50 SPDU O.M.) until approximately 1975, when a slight decrease in the local primary productivity was observed until 2004 (11.43 SPDU O.M.). After this period, we observed an increasing tendency of chlorophyll derivatives, probably due to better preservation of the sedimentary organic matter in the most recent layers (Fig. 2a).

Several authors proposed using Sr/Ca ratio as a possible proxy for the water paleosalinity (Fritz et al. 2018). In this sense, we observed an increasing trend in the phytoplankton-derived organic matter contribution toward the present, accompanied by a decrease in water salinity since ~ 1988. The Khnifiss Lagoon waters are hypersaline, with a gradient of increase toward its innermost compartment (Idrissi et al. 2004); then, an increase in the seawater intake would result in dilution and, consequently, decrease in salinity. The ratios of Si/Ti (Peinerud 2000) also indicate an increase in biogenic silica since ~ 1988, suggesting more microalgae contribution.

Finally, events that resulted in episodic higher energy at the lagoon are highlighted from the median grain size (D₅₀) of the

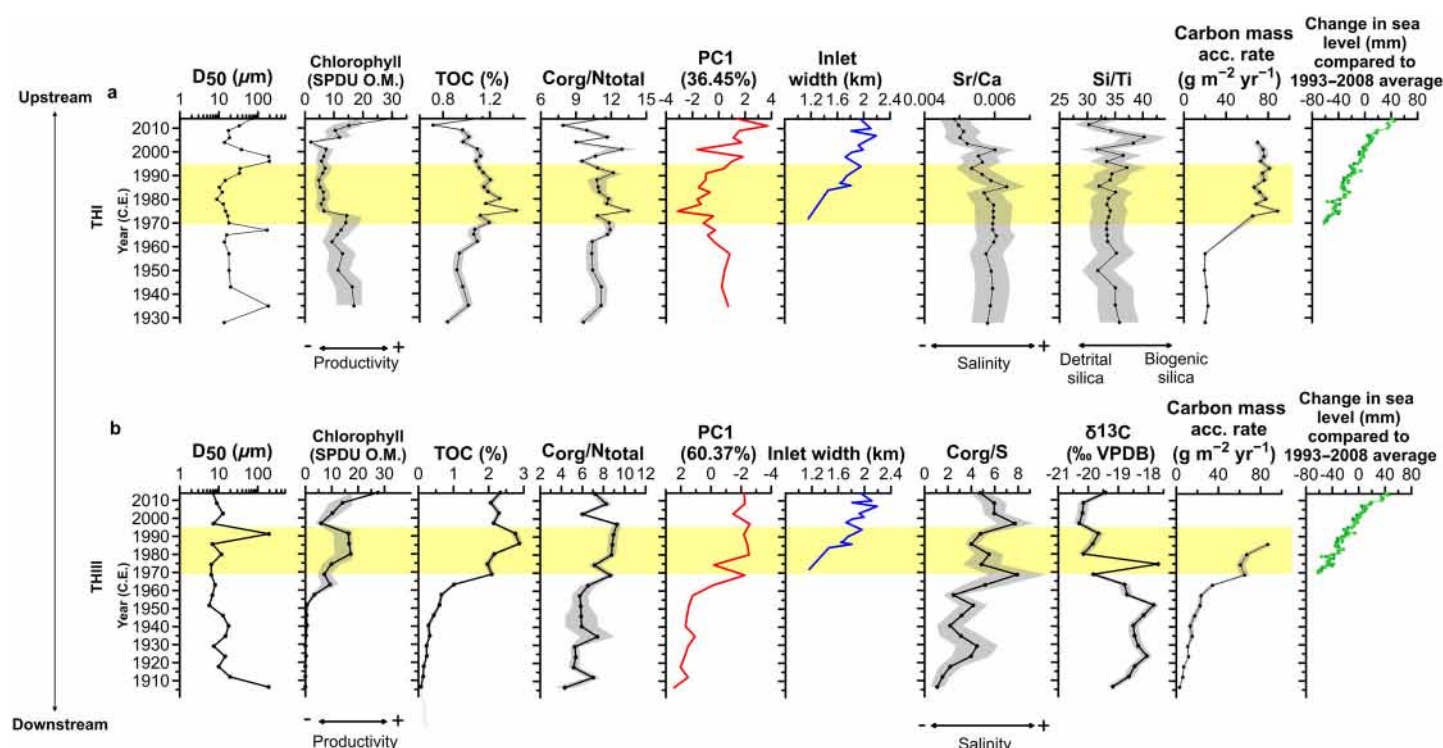


Fig. 2. Time variability of the main geochemical proxies for (a) THI and (b) THIII cores. The yellow-highlighted areas denote the period of more significant changes in the lagoon dynamic due to the interpretation of a successive opening of the lagoon's inlet (~ 1970–1995). The gray-shaded area represents analysis instrumental errors. Blue curves represent the normalized inlet width measured through remote sensing techniques. Red curves represent the PC1 for each sediment core. Green curves represented sea level data from satellite altimeter estimations and by tide gauges measurements.

sediment (Fig. 2a): between 1930 and 1940, around 1965, and about 1995. The spectral analysis of the particle size distribution for core THI indicates the presence of coarse particles for these periods ranging from 150 to 300 μm and containing $> 400 \mu\text{m}$ (Fig. S6a). This variation in the median grain size (D_{50}) (Fig. 2a) may indicate an episodic intensification of the hydrodynamics, supporting the hypothesis of more significant water arrival at this point in the lagoon over the past few years.

THIII core, retrieved closer to the inlet Agoutir, represents the lagoon area with the strongest marine influence and, therefore, under the constant action of currents in and out of the lagoon. The salinity measured at the site on the day of the sampling was 50 PSU, thus revealing a saline gradient that increases toward the upstream, probably due to a longer residence time of the water and consequent higher evaporation rate at that site. The chronological model revealed an accumulation from 1901 to 2014 (Figs. 2b, S7). The sedimentation rate for the THIII core was $\sim 0.35 \text{ cm yr}^{-1}$. Although a possible perturbation in the sedimentation process was noted on the top part of the core, general tendencies were clear enough to allow interpretation. During the recorded period, an increase in TOC, chlorophyll derivatives, and salinity (represented by the C/S ratio; Holland and Turkian 2010) is observed, indicating a general growth in productivity and plant biomass fixation. THIII core is located on a sharp meander margin concerning the principal channel, which

favors sediment/sand accumulation resulting from the very local erosion process. An enhanced deposition in this area would cause the terrain to increase vertically, consequentially leading to a more frequent exposition of the soil and occupation by terrestrial vegetation, turning the $\delta^{13}\text{C}$ signature more negative (Fig. S14). The saltmarsh accretion is a consequence of the deposition of suspended particles during flooding, either minerogenic (allochthonous)—sand, silt, or clay carried in by the tide—or autochthonous accumulation of organic material (from plant roots or aerial parts) or varying combinations of the two (Adam 2016). The sediment deposited may be eroded; however, more sediment is retained as the vegetation density increases. Also, with increasing elevation, the accretion rate declines as the number of flooding tides reaching the terrain at that point decrease (Adam 2016). The bulk particle size distribution of THIII corroborates with this assumption, as it is observed as dominance of fine grain size particles (mainly $< 50 \mu\text{m}$) (Fig. S6b) during most of the record, revealing a low energy environment (Fig. 2b), and as sediment particles settle slowly to the bottom due to plants roots and naturally meandering streams (Weis 2016).

Environmental changes in the Khnifiss Lagoon

In shallow microtidal basins like the Khnifiss Lagoon, characterized by extensive tidal flats and salt marshes, prevailing winds

appear to be important in constraining sediment stabilization and erosion (Fagherazzi et al. 2007; Deng et al. 2018). Tidal flats elevation results from a balance between sediment deposition and resuspension by tidal currents and wind waves (Fagherazzi et al. 2007). Wind waves are also the main cause of salt marsh deterioration through scarp erosion (Fagherazzi and Wiberg 2009). At Venice Lagoon, Italy, winds were found to influence the equilibrium elevation of tidal flats as a result of the relation between wind stress and depth (Fagherazzi et al. 2007). Although processes such as continuous sediment input, varying hydrodynamic and climatic changes prevent the basin's morphology from reaching a long-term stable equilibrium, a relatively large-scale stabilization is expected to be achieved (Deng et al. 2018). In this case, a dynamic equilibrium may be observed between the longitudinal axis of the estuary and the prevailing wind direction (Deng et al. 2018). Thus, explaining the NE position of the Khnifiss Lagoon in consequence of the NE winds, prevailing for the region. This process is valid for wind-dominated systems. For example, at Lake Illawarra, Australia, a similar process occurred, where the estuarine system reached a quasi-equilibrium state, and a planimetric orientation along the prevailing winds was observed (Deng et al. 2018).

Both remote sensing and sedimentological results suggest an enlargement of the lagoon inlet, more pronounced

between the 1970s and the first half of the 1990s. This process led to a great internal water exchange, reaching farther inland portions of the lagoon. In a naturally intact system with low anthropogenic influence, the tidal line is mainly influenced by changes in the: (1) sea level, (2) riverine intake, (3) free inlet area connected to the ocean or sea, and (4) frequency of impacts of extreme events such as storms (Roman et al. 1997). In the case of Khnifiss Lagoon, inserted in a desert environment context, the contribution of water to the lagoon occurs almost exclusively through the Agoutir inlet since (1) precipitation is extremely rare and (2) Ouédri river freshwater is of very low contributions (Dakki and de Ligny 1988). Although storms at sea are infrequent for the region (Dakki and de Ligny 1988), sea-level wind strengthening at the coast and sea-level rise would add significant changes to seawater inflow along the period of the present analysis.

From the remote sensing, we have selected two time intervals that exemplify grand openings of the lagoon inlet (11-1990, Fig. 3a; and 09-2007, Fig. 3b) and other two time intervals of significant narrowing (12-2006, Fig. 3c; and 01-2011, Fig. 3d). We investigated that behavior under different wind predominant directions and intensity overseas. This parameter is related to the wind stress that could potentially affect the coastal sedimentation and coastal sand drifts. When

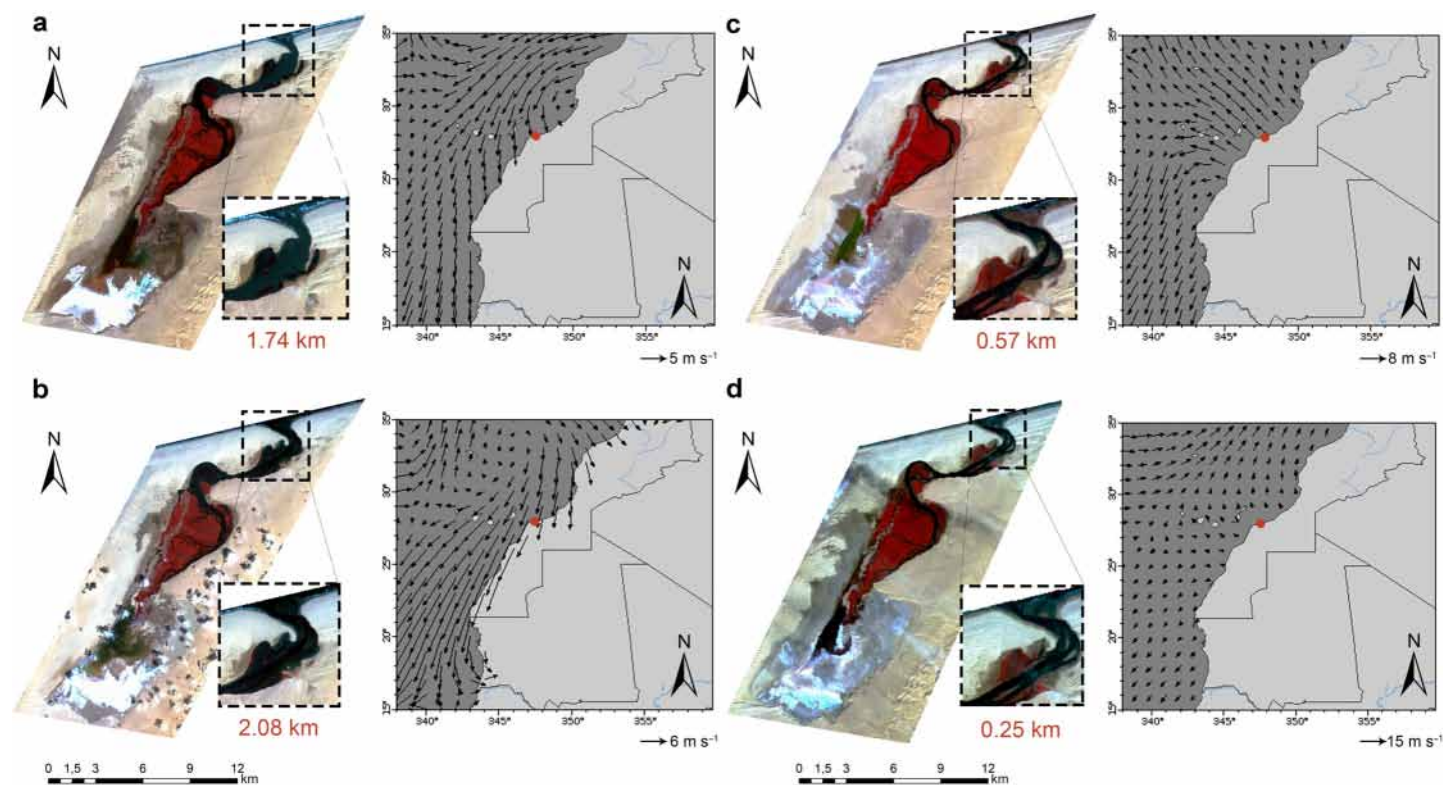


Fig. 3. Exemplification of two time intervals in which there was a wide opening of the inlet (**a** and **b**, 12 November 1990 and 08 September 2007, respectively) and the other two where there was a partial closure (**c** and **d**, 26 December 2006 and 06 January 2011, respectively) through satellite image and wind data at sea level. The red dot represents the studied area of approximated localization. NOAA/NCDC blended daily global 0.25° sea surface winds. Data courtesy of NOAA NCEI.

the inlet width reached up to two kilometers, as in 11-1990 and 09-2007, the main tidal channels enlarged, and the associated vegetation was partially submerged (Fig. 3a,b). During these occasions, sea surface winds data indicated a predominantly wind direction from the ocean to the inland over the lagoon region, reaching the coast obliquely, mainly from the northeastern (Fig. 3a,b). In a condition of restricted opening, with the inlet measuring between 570 and 250 m, as in 12-2006 and 01-2011, the tidal channels have become narrower and the vegetation more exposed, while the predominant sea surface winds blew nearly the opposite direction from the continent to the ocean (Fig. 3c,d). The observed changes in wind vectors of Fig. 3 suggest that the lagoon is under the influence of the positioning of the cyclone (over tropical North Africa < 15°N) and anticyclone systems (Azores high and the one at the subtropical Sahara, 27–32°N, over Algeria) (Rodríguez et al. 2015) that modulates the regional wind redistribution.

The action of winds on coastal ocean waters can “induce” temporary changes in the water levels of estuaries (Rozas 1995). From the above, we believe that Khnifiss Lagoon water levels respond to such a process driven by the wind on the coast. In summary, prevailing ocean-continent winds increase the filling velocity, while emptying velocities (ebb velocities) are increased when winds blow from the continent to the ocean (Morton 1994). For the Khnifiss Lagoon, it is reported that the emptying of the lagoon occurs faster than the filling due to variations in the current, which is more pronounced during the first situation (Idrissi et al. 2004). Therefore, the emptying currents are responsible for more mobilization of fine sediments from the lagoon to the continental shelf.

The maintenance of the inlet opening condition seems to be a complex process based on the balance of the filling current that removes the accumulated sediments at the proximity of the inlet and the exported amounts from the lagoon during its emptying. In inlets dominated by the ebb tide, such as the Agoutir, the transport of sediments toward the interior of the lagoon to the so-called back-barrier occurs when there is an increase in wave energy on the coast (FitzGerald 1988), generally associated with increased surface wind stress. Both our remote sense analysis and our geochemical data retrieved from the sediment cores show no evidence of enclosure or ephemeral conditions of the lagoon since ~ 1900 C.E. However, a reduction of the inlet extension was observed. According to Kjerfve and Magill's (1989) classification of coastal lagoons, the Khnifiss Lagoon is considered a choked lagoon characterized by one or more long and narrow entrance channels. Depending on the direction and duration of wind stress together with the direction and degree of wave energy, which determines the potential of coastal erosion and coastal transport of sediments, choked lagoon inlets may be enlarged or narrowed by sediment deposition at the entrance (Bird 1994). Impacts on the hydrological and ecological functions are expected due to this dynamic.

For the innermost compartment of the lagoon, herein represented by the THI sediment core, the greater continuous opening process of the inlet, presumed to have occurred between 1970 and 1995, caused the increased water exchange and sedimentation rates. In the sediment core, it is represented by a predominance of biogenic silica, a decrease in organic carbon resulting from the predominance of phytoplankton biomass, higher productivity, and a reduction in salinity that lasted at least 25 yr (1970–1995). After 1999, THI site experienced its lower salinity values, a greater predominance of biogenic silica linked to the predominance of phytoplankton biomass, and higher productivity, indicating that the water continued to arrive in these portions until the present day. Overall, we deduced that at the THI site, migration of habitats took place, where the increased arrival of water, and a consequent change in tide line, caused a predominance of pioneer vegetation, characteristic of intertidal environments, which are under more extended periods of submergence. Based on the $\delta^{13}\text{C}$ vs. C/N diagram (Fig. S14), we interpret that along the recorded time, there has been a relative change in the predominant vegetation, from lower marsh one giving away to others adapted to more frequent submersion periods, such as *Spartina maritima* and *Z. noltii*. According to Esteves (2016), coastal ecosystems vary dynamically to adjust to new oceanographic and meteorological conditions such as short- and long-term sea-level fluctuations. The tidal range is one of the main factors in the shift of habitats toward land, whose zoning will reflect the tolerance of different plant species to flooding.

For the zones closer to the lagoon inlet, represented by the THIII sediment core, the alleged higher entry of seawater, evidenced by the increasing C/S ratio, could have caused more transport of marine and eroded materials from the lagoon borders to the system. The above process favored a decrease in the sedimentation rates and an increase in the terrestrial input, revealed by the Ti/Ca ratio and the increase in detrital silica, as seen in the Si/Ti ratio. Therefore, during the increased inlet size phases, more significant redistribution of sediments into the lagoon leads to its accumulations downstream, causing a vertical accretion in terrain elevation and exposition. Hence, the soil exposition caused by the sediment accumulation led to a change in the predominant vegetation from a mostly phytoplanktonic contribution to a marsh environment, characterized by periodically submersion and exposure cycles. The propagation of local vegetation is depicted by the increase in the TOC and chlorophyll derivatives. Recently (~ 1997), though, another scenario is portrayed, when lower values accompany a sedimentation rate increase in the $\delta^{13}\text{C}$ signature, a decrease in TOC, and an increase in chlorophyll derivatives. This suggests a local decrease in the terrain and, thus, returning to a submerged predominant environment condition, although more productive than the previous (1901–1960).

A PCA was performed for each core data, including their more representative geochemical proxies and sedimentation rates (Figs. 2, S8). The three first principal components (PCs)

represented, cumulatively, 78.4%, and 86.7% of the data variance for THI and THIII, respectively. The first principal component (PC1) accounted for 36.2% for THI and 64.0% for THIII for the observed variance. PC1 temporal behavior at both sediment cores (red curves in Fig. 2) presented high similarity concerning the inlet width.

Therefore, the PC1 reflects that the most important changes in the lagoon were driven by the inlet dynamics and the consequent redistribution of seawater in the inner portions of the lagoon. Bringing this understanding to the past decades, changes between the beginning of the sedimentary record, ~ 1928 to 1972, can be interpreted as a more extended period of water residence due to ineffective seawater transport at the inner portions of the lagoon. We observe lower sedimentation rates, higher contribution of detrital silica, higher salinity, and the predominance of grains < 20 μm , indicating lower hydrodynamics at the THI site. At the near inlet zone, we observed lower marine influence and silica detritus predominance—also less vegetation coverage, as indicated by THIII TOC and chlorophyll derivatives time series.

For the Khnifiss Lagoon, inlet restrictions that probably occurred at the beginning (bottom part) of the sedimentary record and reflected by the PC1 were associated with lower sedimentation rates, higher salinity, and lower hydrodynamics. The use of process-based soil elevation models for estuaries throughout California showed that in scenarios with little or no fluvial influx, inlet closures or restrictions can cause a decrease in marsh elevation (Thorne et al. 2021). In this case, low accretion rates were expected due to the diminishment of tidal sediment fluxes, as also observed in the beginning (bottom part) of our record. Like the paleoenvironment changes at the Khnifiss Lagoon, at Lake Illawarra (Australia)—a coastal lagoon connected to the ocean by a tidal inlet and with low river inflow—changes in the inlet had a consequence for the system hydrodynamics (Sloss et al. 2005). Restrictions in the lagoon's inlet were associated with a reduction in water movement and circulation, changes from sand- to mud-dominated strata, and higher salinity. However, when the connection with the ocean was more efficient, deposition of medium to coarse-grained sand was observed, and a higher energy system was assumed (Sloss et al. 2005). Similar to reports by Saintilan et al. (2016), the opening regime of estuarine entrances observed in southern California and southeast Australia may effectively change the vegetation structure and the ecosystem geochemistry and may promote carbon sequestration and encourage the recruitment of marine fish larvae.

The Khnifiss Lagoon and its potential as a carbon sink

In a climate change scenario and rising atmospheric CO_2 concentration, carbon sequestration effectively mitigates the Earth's surface geochemical imbalances (IPCC 2014). Marine organisms play an important part in carbon sequestration (Duarte et al. 2013). Vegetated coastal habitats, especially, have been pointed as important carbon sinks, supporting relevant

rates of organic carbon burial on a global level (Duarte et al. 2013). Recurrent coastal upwelling is one of the main factors for higher productivity, by contributing to nutrient input and consequence increase in carbon fluxes (McGregor et al. 2007; Montero et al. 2007). The region off the coast of the Khnifiss Lagoon is part of the Cape Ghir upwelling system, an important and persistent upwelling cell along the NW African coast (McGregor et al. 2007). Estimations of the carbon mass accumulation rate for the Khnifiss Lagoon averaged from 59.30 ± 25.18 to 24.97 ± 25.35 $\text{g C m}^{-2} \text{yr}^{-1}$ for THI and THIII cores, respectively (Fig. 2). An increasing trend in the carbon flux is observed for both cores, following the TOC and chlorophyll content increased trend. Consistent with a higher phytoplanktonic contribution, the observed changes indicate the Khnifiss Lagoon's important role as a carbon sink. For THIII core, for example, the average values in the sediments changed from 7.32 $\text{g C m}^{-2} \text{yr}^{-1}$, for the core bottom (1901–1923), to 69.70 $\text{g C m}^{-2} \text{yr}^{-1}$ in its uppermost part (1923–1985), while for THI, values average were stable around 74.13 $\text{g C m}^{-2} \text{yr}^{-1}$ since ~ 1970. For comparison, at San Quintín Bay, a shallow lagoon in Mexico, carbon burial estimations revealed an average carbon burial rate between 29.7 and 42.2 $\text{g C m}^{-2} \text{yr}^{-1}$ from sediment cores retrieved at the saltmarsh and 57.9 and 58.5 $\text{g C m}^{-2} \text{yr}^{-1}$ from the ones recovered at the seagrass dominated area (Cuellar-Martinez et al. 2019). For the Indian Ocean upwelling region off Java and Sumatra, Indonesia, the maximum organic carbon accumulation rates were between 5.2 and 10.4 $\text{g C m}^{-2} \text{yr}^{-1}$ (Baumgart et al. 2010). For the Peruvian coast, ~ 15°S, a highly productive upwelling region, estimations of surface sediment organic carbon accumulation rates were between 40 and 70 $\text{g C m}^{-2} \text{yr}^{-1}$ (Henrichs and Farrington 1984).

Considering their insertion in an arid environment, there coastal wetlands provide surprisingly high levels of regional ecosystem services that support fisheries (Aburto-Oropeza et al. 2008), biodiversity (Sievers et al. 2019), and carbon sequestration (Adame et al. 2018). The presented comparisons point to the relevance of the Khnifiss Lagoon as a carbon burial ecosystem and highlight the need for more data on organic carbon burial rates for the poorly studied tidal flat-saltmarsh ecosystems (Cuellar-Martinez et al. 2019). An improved understanding of the ecology, process, and dynamics of coastal vegetated wetlands in arid environments is necessary to protect and maintain their valued ecosystem services (Adame et al. 2021).

Regional responses to climate changes

From wind databases derived from remote sensing, we observed an intensification of trade winds from the northeast to the Khnifiss region during the 1960s when wind speed on the continental shelf in front of the inlet was 5.0 m s^{-1} on average. During the 1970s, it increased to 5.5 m s^{-1} , and from the 1990s onward, it turned to be 6.0 m s^{-1} on average (Figs. S9, S10). Due to the east-to-west alignment of the coast

and an oblique action of the northeast trade winds, a high frequency of these winds favors the opening of the Khnifiss Lagoon inlet. It, therefore, provides an increase in the marine influence in this coastal environment. Thus, in a situation of wind strengthening under the above conditions, the seawater input in the lagoon would be favored, which corroborates the interpretations derived from both sedimentary records and satellite data.

The NCEP/NCAR Reanalysis surface winds analysis (Fig. S11) displays an increase in wind speed during NAO + (positive values of NAO) years, indicating a relationship between the NAO index and the wind speed in the continental shelf in front of the Khnifiss Lagoon. Most important is that NAO has an inverse correlation to the zonal wind. In periods of NAO +, winds are strengthening in an east-to-west direction (Fig. S12). Models based on CMIP5 scenarios and RCP 4.5 simulations projected a slightly positive future trend for the NAO (Stephenson et al. 2006). The observed increase in the carbon flux for the Khnifiss Lagoon is a consequence of the strengthening in the NE winds reaching off coast. The result is the opening of the lagoon's inlet and the increased entering of nutrient-rich water into the system, as discussed previously. The strengthening of the alongshore winds also increases the upwelling in the region (McGregor et al. 2007). An upwelling intensification off the NW coast for the 20th century is confirmed through Sea Surface Temperature records from Moroccan sediment cores and is expected to continue intensifying in the future (McGregor et al. 2007). All this together points to a potential strengthening of the Khnifiss Lagoon as a carbon sink in the future. Given the importance of coastal vegetated wetlands and their potential role in carbon sequestration, further understanding of climate feedbacks in upwelling regions and the role of coastal environments is imperative.

Although in the Khnifiss vicinity no long-term tide gauge data exist, for the last 40 yr, it is estimated that sea level had risen around 10 cm in North Tropical Atlantic according to satellite altimeter data (Church and White 2011) and measures by tide gauges (Caldwell et al. 2015) (Fig. 2). Models and observations have evidenced potential effects to coastal communities due to the combined effect of storms, high astronomical tide, and sea-level rise in all IPCC scenarios (McInnes et al. 2003). Their model points to a considerable impact on coastal zones, especially regarding two aspects: floods and shoreline modification. Therefore, for Khnifiss, which presents a predominantly sandy inlet structure and an apparent relation between seawater inflow in the lagoon and coastal winds, we do not discard that modern sea-level rise has a synergistic contribution to the local hydrological dynamics.

Coastal narrowing in arid environments

Coastal wetlands, an essential source of ecosystem services, have suffered a loss of area over time so that a better understanding of this process is vital. Wetlands tend to transition

upward and thus adjust their position concerning the new tidal limit and persist or even expand during these scenarios due to rising water levels, either locally or at sea level (Schuerch et al. 2018). This migration depends on hydrological, sedimentological, and ecological factors (Rogers 2021). The availability of accommodation space is then studied as a way to conceptualize coastal wetlands' response to changes in the tidal limit. The accommodation space is related to the vertical and lateral space available for the accumulation of fine sediment (mineral and organic) and organic material that allows the consequent colonization by vegetation (Schuerch et al. 2018; Rogers 2021). Coastal wetland vulnerability can be accessed by comparing the rates of substrate elevation change to rates of changes in the tidal limit rise. However, the actually estimated vulnerability may be overstated due to the lack of adequate explanation regarding the resilience provided by mineral and organic sediments in terms of providing accommodation space and substrate elevations in situ (Rogers 2021). The available accommodation space is limited by boundary conditions such as sea level, basement geology, altered hydrodynamic energy, and human-made barriers (Pontee 2013; Rogers 2021). These conditions define the spatial boundaries in which processes operate and limit the potential area for accommodation space occurrence (Cowell and Thom 1994). If there is no or low limitation in this aspect, the vegetation tends to colonize the environment quickly, and there is an expansion of the saltmarsh area. However, if there is a substantial limitation in the accommodation space, the final balance between loss and gain of the area will tend to be negative (Schuerch et al. 2018).

This phenomenon, presented in Fig. 4 as “migration of habitats towards the interior,” compensates for the loss of area in the portions closest to the ocean by allowing expansion in more continental zones. The geomorphological response of vegetated coastal wetlands is a complex dynamic involving feedback between hydrodynamics, sedimentation, and plant productivity (Krauss et al. 2014) and their interaction with landscape-scale dynamics and localized factors (Rogers 2021). Given that coastal wetlands occupy a great variety of environments with a specific combination of shoreline morphologies, local geology, climate, ecological function, and impacts, a generalized projection for their response to changes such as sea-level rise is far from ideal. It is reasonable then to assume that coastal wetland response and adaption will be spatially variable once vegetation zonation shifts according to these factors and their combined impact on potential habitats upward expansion.

For coastal wetlands inserted in an arid or semi-arid environment, we propose that the accommodation space availability related to the surrounding geology—with dunes and rocky reg desert pavement—and local climate exerts a much stronger control over the persistence of the vegetation, especially from the upper marsh, when compared to the sea-level rise or altered hydrodynamic energy. This proposal is especially true for the Khnifiss Lagoon, located in a pristine environment

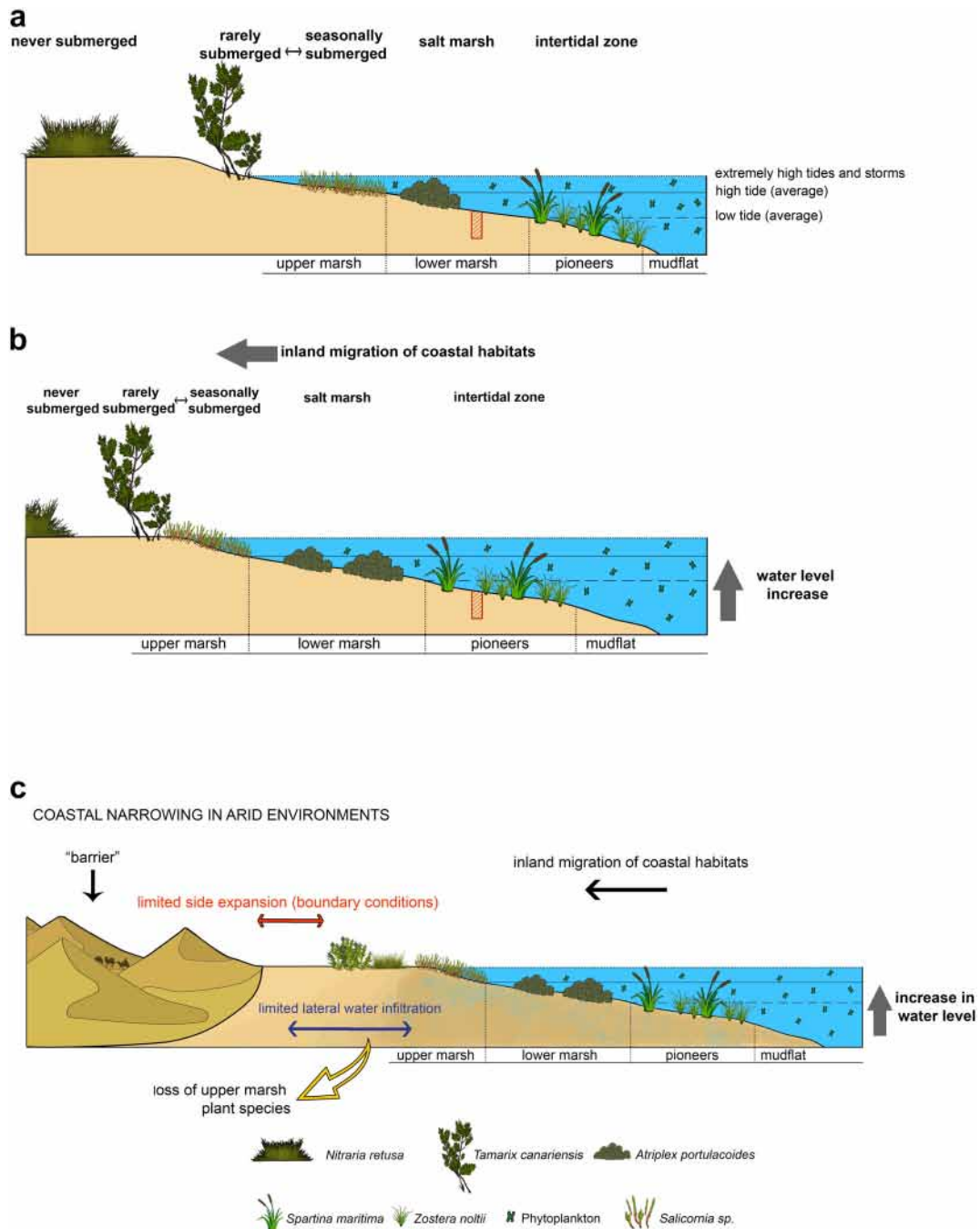


Fig. 4. Conceptual model of a coastal narrowing in arid environments, as supposed for the Khnifiss Lagoon. **(a)** Scenario representation of a sediment core (red hashed rectangle) extracted in a lower marsh environment, in which soils are periodically submerged. **(b)** In case of water level rise, related to the tidal limits, the previously cited local environment would have instead sheltered pioneer vegetation, as *S. maritima*, as a result of the inland migration of the habitat. Diagrams **a** and **b** are in scale. **(c)** In arid areas, changes in the tidal line with limited accommodation space could cause the loss of the upper marsh vegetation and generate a net loss of wetlands.

with low human impact. Pontee (2013) delimits the concept of “coastal squeeze,” which can be defined as the loss of intertidal habitats due to rising sea levels along the shoreline limited by anthropic structures. Although in the case of the Khnifiss Lagoon, there are no physical human-made physical barriers

that would prevent a possible vertical and lateral expansion of habitats, the surrounding desert climate itself and the landscape consisting of a desert plateau on the left bank and transverse dunes on the right would act as a barrier, making the term “coastal narrowing” more suitable (Pontee 2013).

A subsequent narrowing of coastal areas could cause a decrease in vegetation coverage for the Khnifiss Lagoon, with the loss of vegetation typical of the upper marsh impacting all the biota that forages and shelters there. The increase in current, caused by changes in channel and bank position due to changes in the inlet, is a potential cause for erosion of the most oceanic portions and lateral loss of intertidal habitats (Pontee 2013). Further restrictions on lateral vegetation expansion may result from possible adverse conditions in soil conditions, geomorphologic characteristics (Schuerch et al. 2018), and here, we add, climatic conditions. Thus, for arid coastal wetlands, as in the case of Khnifiss Lagoon, changes in the tidal limit influence the vegetation zonation, which, due to its insertion in an arid climate, with insignificant fluvial hydrological inputs and surrounded by dunes, has its accommodation space limited (*see* Fig. S13 for flow diagram). Such limitation restricts the migration of habitats, causing the loss of the upper marsh vegetation and generates a net loss of wetlands, as represented in Fig. 4, whose lateral and vertical expansion is influenced by limited aquatic infiltration due to the extreme climatic conditions of the region and the sandy substrate. Degradation of arid coastal wetlands has been related to vegetation salinity tolerance and the fact that changes in hydrology, climate, or nutrient loads, even in small scale, can have a great impact on its persistence (Lovell et al. 2009; Adame et al. 2021).

Conclusions

The use of remote sensing combined with geochemical and physical analysis of lacustrine sediment cores improved our knowledge of the sedimentary history of Khnifiss Lagoon since 1901. Through remote sensing, it was possible to quantitatively describe the increase of the Agoutir inlet between 1972 and 1994, accompanied by a greater meandering character of the tidal channels. Such change greatly impacted the lagoon geochemistry, sedimentation, vegetation succession, and, therefore, the lacustrine ecosystem overall. The presence of inlet(s) in coastal lagoons ensures mass exchange between it and the ocean, having great natural and environmental importance. Thus, the knowledge of the behavior and evolution of inlets is essential to understand and enable a particular prediction about the consequences of extreme natural events.

The maintenance of the inlet opening condition seems to be a complex process; changes in its position and length have impacts on the hydrological and ecological functions. For the case of the Khnifiss Lagoon, whose inlet is dominated by the ebb tide, the intensity and direction of the winds on the coast at surface level acts on the inlet by increasing the ocean allochthonous material and nutrients exportation toward the interior of the lagoon as well as intensifying the filling current. Great inlet opening was observed when the wind blew predominantly from the ocean to the inland over the lagoon

region, reaching the coast obliquely, mainly from the north-eastern direction.

Vegetated coastal habitats, especially, have been pointed as important carbon sinks. Carbon accumulation rate estimations for the Khnifiss Lagoon revealed an increasing tendency for both of its analyzed zones, and high values, up to $88.65 \text{ g C m}^{-2} \text{ yr}^{-1}$, were observed in the most recent sediment layers. These estimations indicate the great potential of the Khnifiss Lagoon as a carbon burial ecosystem and highlight the need for more carbon flux studies in tidal flat-saltmarsh ecosystems.

A relation between the NAO index and the wind speed in the continental shelf in front of the Khnifiss Lagoon was observed; in periods of NAO+, winds are strengthening in an east-to-west direction. An intensification of northeast trade winds was observed since the 1970s through wind databases, and it is interpreted as the main cause for the observed inlet dynamics. Wind intensification in the coast is also related to intensification in the upwelling and may have favored carbon flux increases. We believe that modern sea-level rise has a synergistic contribution to the local hydrological dynamics.

The distribution of the tidal vegetation follows a zoning pattern linked to the tolerance of the plants to flooding and salinity. Although the tidal flats are highly dynamic environments, in a possible future scenario of tidal line displacement, it is expected that as a consequence, there will be a loss of upper marsh vegetation. This conclusion is based on the fact that, due to its insertion in a desert climate, the Khnifiss Lagoon becomes highly prone to the process of coastal narrowing. Herein, we propose that this process occurs due to the combination of local geology (dunes and rocky reg desert pavement) and local climate, which act as boundary conditions in limiting the accommodation space and could refrain from expanding the upper tidal vegetation toward the interior.

The rare coastal lagoons and wetlands at Northern Sahara are key environments related to natural services sustainability. Here, we demonstrated that parameters as the regional wind structure, driven by known climate changes, can deeply impact the lagoon hydrodynamics and biogeochemical cycles. This observation exemplifies the great sensitivity of Khnifiss Lagoon to large-scale climatic processes.

Data availability statement

All data used in this work are provided in the Supplementary Information and at PANGAEA Data Publisher under the id PDI-25609 (<https://doi.pangaea.de/10.1594/PANGAEA.925346>).

References

- Aburto-Oropeza, O., E. Ezcurra, G. Danemann, V. Valdez, J. Murray, and E. Sala. 2008. Mangroves in the Gulf of California increase fishery yields. *Proc. Natl. Acad. Sci.* **105**: 10456–10459. doi:[10.1073/pnas.0804601105](https://doi.org/10.1073/pnas.0804601105)

- Adam, P. 2016. Saltmarshes, p. 515–535. *In* M. J. Kennish [ed.], *Encyclopedia of estuaries*. Encyclopedia of earth sciences series. Springer.
- Adame, M. F., E. Najera, C. E. Lovelock, and C. J. Brown. 2018. Avoided emissions and conservation of scrub mangroves: Potential for a Blue Carbon project in the Gulf of California, Mexico. *Biol. Lett.* **14**: 20180400. doi:10.1098/rsbl.2018.0400
- Adame, M. F., R. Reef, N. S. Santini, E. Najera, M. P. Turschwell, M. A. Hayes, P. Masque, and C. E. Lovelock. 2021. Mangroves in arid regions: Ecology, threats, and opportunities. *Estuar. Coast. Shelf Sci.* **248**: 106796. doi:10.1016/j.ecss.2020.106796
- AEFCS. 1996. Plan Directeur des Aires Protégées du Maroc: Vol. 3. Sites d'Intérêt Biologique et Ecologique littoraux, Admin. Eaux et Forêts & Conservation des Sols, BCEOM/SECA.
- El Agbani, M. A., M. Fekhaoui, A. Bayed, and J. R. Schouten. 1988. The Khnifiss Lagoon and adjacent waters: Hydrology and hydrodynamics, p. 17–26. *In* M. Dakki and W. De Ligny [eds.], *The Khnifiss Lagoon and its surrounding environment* (Province of La'youne, Morocco). Travaux de l'Institut Scientifique Chérifien et de la Faculté des Sciences.
- Barua, P., S. H. Rahman, S. Barua, and I. M. M. Rahman. 2020. Climate change vulnerability and responses of fisherfolk communities in the south-eastern coast of Bangladesh. *Water Conserv. Manag.* **4**: 20–31. doi:10.26480/wcm.01.2020.20.31
- Baumgart, A., T. Jennerjahn, M. Mohtadi, and D. Hebbeln. 2010. Distribution and burial of organic carbon in sediments from the Indian Ocean upwelling region off Java and Sumatra, Indonesia. *Deep-Sea Res. Part I Oceanogr. Res. Pap.* **57**: 458–467. doi:10.1016/j.dsr.2009.12.002
- Berrisford, P., and others. 2011. The ERA-Interim archive Version 2.0. ERA Report Series 1.
- Bird, E. C. F. 1994. Physical setting and geomorphology of coastal lagoons, p. 9–39. *In* B. Kjerfve [ed.], *Coastal lagoon processes*. Elsevier Science BV.
- Caldwell, P. C., M. A. Merrifield, and P. R. Thompson. 2015. Sea level measured by tide gauges from global oceans — the Joint Archive for Sea Level holdings (NCEI Accession 0019568), Version 5.5, NOAA National Centers for Environmental Information, Dataset. doi:10.7289/V5V40S7W
- Church, J. A., and N. J. White. 2011. Sea-level rise from the late 19th to the early 21st century. *Surv. Geophys.* **32**: 585–602. doi:10.1007/s10712-011-9119-1
- Congalton, R. G., and K. Green. 2019. *Assessing the accuracy of remotely sensed data*, 3rd ed. CRC Press.
- Cowell, P., and B. Thom. 1994. Morphodynamics of coastal evolution, p. 33–86. *In* R. Carter and C. Woodroffe [eds.], *Coastal evolution: Late quaternary shoreline morphodynamics*. Cambridge Univ. Press.
- Crossland, C. J., H. H. Kremer, H. Lindeboom, J. I. M. Crossland, and M. D. A. Le Tissier. 2005. Coastal fluxes in the anthropocene - the land-ocean interactions in the coastal zone project of the International Geosphere-Biosphere Programme. Springer, Berlin, Heidelberg
- Cuellar-Martinez, T., A. C. Ruiz-Fernández, J.-A. Sanchez-Cabeza, L.-H. Pérez-Bernal, and J. Sandoval-Gil. 2019. Relevance of carbon burial and storage in two contrasting blue carbon ecosystems of a north-east Pacific coastal lagoon. *Sci. Total Environ.* **675**: 581–593. doi:10.1016/j.scitotenv.2019.03.388
- Dakki, M., and W. de Ligny. 1988. The Khnifiss lagoon and its surrounding environment (Province of L'ayoune, Morocco). Travaux Institut Scientifique de Rabat.
- Day, J. W., and others. 2008. Consequences of climate change on the ecogeomorphology of coastal wetlands. *Estuar. Coasts* **31**: 477–491. doi:10.1007/s12237-008-9047-6
- Deng, J., B. G. Jones, K. Rogers, and C. D. Woodroffe. 2018. Wind influence on the orientation of estuarine landforms: An example from Lake Illawarra in southeastern Australia. *Earth Surf. Process. Landf.* **43**: 2915–2925. doi:10.1002/esp.4459
- Duarte, C. M., I. J. Losada, I. E. Hendriks, I. Mazarrasa, and N. Marbà. 2013. The role of coastal plant communities for climate change mitigation and adaptation. *Nat. Clim. Change* **3**: 961–968. doi:10.1038/nclimate1970
- Erwin, K. L. 2009. Wetlands and global climate change: The role of wetland restoration in a changing world. *Wetl. Ecol. Manag.* **17**: 71–84. doi:10.1007/s11273-008-9119-1
- Esteves, L. S. 2016. Coastal squeeze. *Encyclopedia of Earth Sciences Series*. Springer.
- Fagherazzi, S., C. Palermo, M. C. Rulli, L. Carniello, and A. Defina. 2007. Wind waves in shallow microtidal basins and the dynamic equilibrium of tidal flats. *J. Geophys. Res.* **112**: F02024. doi:10.1029/2006JF000572
- Fagherazzi, S., and P. L. Wiberg. 2009. Importance of wind conditions, fetch, and water levels on wave-generated shear stresses in shallow intertidal basins. *J. Geophys. Res.* **114**: F03022. doi:10.1029/2008JF001139
- FAO. 2018. *The state of world fisheries and aquaculture - meeting the sustainable development goals*. Food and Agriculture Organization.
- FitzGerald, D. M. 1988. Shoreline erosional-depositional processes associated with tidal inlets. *Hydrodyn. Sediment Dyn. Tidal Inlets* **29**: 186–225. doi:10.1007/978-1-4757-4057-8_11
- Fritz, M., and others. 2018. Regional environmental change versus local signal preservation in Holocene thermokarst lake sediments: A case study from Herschel Island, Yukon (Canada). *J. Paleolimnol.* **60**: 77–96. doi:10.1007/s10933-018-0025-0
- Hammada, S. 2007. Etudes sur la végétation des zones humides du Maroc. Univ. Mohammed V – Agdal.
- Henrichs, S. M., and J. W. Farrington. 1984. Peru upwelling region sediments near 15°S. 1. Remineralization and accumulation of organic matter. *Limnol. Oceanogr.* **29**: 1–19. doi:10.4319/lo.1984.29.1.0001
- Holland, H. D., and K. K. Turekian. 2010. *In* H. D. Holland and K. K. Turekian [eds.], *Readings from the treatise on geochemistry*, 1st ed. Elsevier.

- Huete, A. 1988. A soil-adjusted vegetation index (SAVI). *Remote Sens. Environ.* **25**: 295–309. doi:[10.1016/0034-4257\(88\)90106-X](https://doi.org/10.1016/0034-4257(88)90106-X)
- Idrissi, J. L., A. Orbi, F. Zidane, K. Hilmi, F. Sarf, Z. Massik, and A. Makaoui. 2004. Organisation et fonctionnement d'un écosystème côtier du Maroc: la lagune de Khnifiss. *Rev. Sci. l'eau* **17**: 447–462. doi:[10.7202/705542ar](https://doi.org/10.7202/705542ar)
- IPCC. 2014. Climate change 2014 synthesis report.
- Julien, P. Y. 2018. River equilibrium, in river mechanics.
- Kalnay, E., and others. 1996. The NCEP/NCAR 40-year reanalysis project. *Bull. Am. Meteorol. Soc.* **77**: 437–471. doi:[10.1175/1520-0477\(1996\)077<0437:TNYRP>2.0.CO;2](https://doi.org/10.1175/1520-0477(1996)077<0437:TNYRP>2.0.CO;2)
- Kjerfve, B., and K. Magill. 1989. Geographic and hydrodynamic characteristics of shallow coastal lagoons. *Mar. Geol.* **88**: 187–199. doi:[10.1016/0025-3227\(89\)90097-2](https://doi.org/10.1016/0025-3227(89)90097-2)
- Krauss, K. W., K. L. McKee, C. E. Lovelock, D. R. Cahoon, N. Saintilan, R. Reef, and L. Chen. 2014. How mangrove forests adjust to rising sea level. *New Phytol.* **202**: 19–34. doi:[10.1111/nph.12605](https://doi.org/10.1111/nph.12605)
- Lovelock, C. E., M. C. Ball, K. C. Martin, and I. C. Feller. 2009. Nutrient enrichment increases mortality of mangroves R. Thompson [ed.]. *PLoS One* **4**: e5600. doi:[10.1371/journal.pone.0005600](https://doi.org/10.1371/journal.pone.0005600)
- Macreadie, P. I. 2020. The future of blue carbon science. *Nat. Commun.* **10**: 1–13. doi:[10.1038/s41467-019-11693-w](https://doi.org/10.1038/s41467-019-11693-w)
- McFadden, L., T. Spencer, and R. J. Nicholls. 2007. Broad-scale modelling of coastal wetlands: What is required? *Hydrobiologia* **577**: 5–15. doi:[10.1007/s10750-006-0413-8](https://doi.org/10.1007/s10750-006-0413-8)
- McGregor, H. V., M. Dima, H. W. Fischer, and S. Mulitza. 2007. Rapid 20th-century increase in coastal upwelling off northwest Africa. *Science (80-)* **315**: 637–639. doi:[10.1126/science.1134839](https://doi.org/10.1126/science.1134839)
- McInnes, K. L., K. J. E. Walsh, G. D. Hubbert, and T. Beer. 2003. Impact of sea-level rise and storm surges in a coastal community. *Nat. Hazards* **30**: 187–207. doi:[10.1023/A:1026118417752](https://doi.org/10.1023/A:1026118417752)
- Möller, I., and others. 2014. Wave attenuation over coastal salt marshes under storm surge conditions. *Nat. Geosci.* **7**: 727–731. doi:[10.1038/NGEO2251](https://doi.org/10.1038/NGEO2251)
- Montero, P., G. Daneri, L. A. Cuevas, H. E. González, B. Jacob, L. Lizárraga, and E. Menschel. 2007. Productivity cycles in the coastal upwelling area off Concepción: The importance of diatoms and bacterioplankton in the organic carbon flux. *Prog. Oceanogr.* **75**: 518–530. doi:[10.1016/j.pocean.2007.08.013](https://doi.org/10.1016/j.pocean.2007.08.013)
- Morton, R. A. 1994. Texas barriers, p. 75–114. *In* R. A. Davis [ed.], *Geology of holocene barrier island systems*. Springer.
- Peinerud, E. K. 2000. Interpretation of Si concentrations in lake sediments: Three case studies. *Environ. Geol.* **40**: 64–72. doi:[10.1007/PL00013330](https://doi.org/10.1007/PL00013330)
- Pontee, N. 2013. Defining coastal squeeze: A discussion. *Ocean Coast. Manag.* **84**: 204–207. doi:[10.1016/j.ocecoaman.2013.07.010](https://doi.org/10.1016/j.ocecoaman.2013.07.010)
- Rey, J. R. 2016. Coastal wetlands, p. 160–164. *In* M. J. Kennish [ed.], *Encyclopedia of estuaries*. Springer.
- Richir, J., S. Bouillon, S. Gobert, M. W. Skov, and A. V. Borges. 2020. Editorial: Structure, functioning and conservation of coastal vegetated wetlands. *Front. Ecol. Evol.* **8**: 1–4. doi:[10.3389/fevo.2020.00134](https://doi.org/10.3389/fevo.2020.00134)
- Robbins, J. A., and D. N. Edgington. 1975. Determination of recent sedimentation rates in Lake Michigan using Pb-210 and Cs-137. *Geochim. Cosmochim. Acta* **39**: 285–304. doi:[10.1016/0016-7037\(75\)90198-2](https://doi.org/10.1016/0016-7037(75)90198-2)
- Rodríguez, S., E. Cuevas, J. M. Prospero, A. Alastuey, X. Querol, J. López-Solano, M. I. García, and S. Alonso-Pérez. 2015. Modulation of Saharan dust export by the North African dipole. *Atmos. Chem. Phys.* **15**: 7471–7486. doi:[10.5194/acp-15-7471-2015](https://doi.org/10.5194/acp-15-7471-2015)
- Rogers, K. 2021. Accommodation space as a framework for assessing the response of mangroves to relative sea-level rise. *Singap. J. Trop. Geogr.* **42**: 163–183. doi:[10.1111/sjtj.12357](https://doi.org/10.1111/sjtj.12357)
- Roman, C. T., J. A. Peck, J. R. Allen, J. W. King, and P. G. Appleby. 1997. Accretion of a New England (U.S.A.) salt marsh in response to inlet migration, storms, and sea-level rise. *Estuar. Coast. Shelf Sci.* **45**: 717–727. doi:[10.1006/ecss.1997.0236](https://doi.org/10.1006/ecss.1997.0236)
- Royaume du Maroc. 2015. Portrait de secteur de pêche maritime au Maroc.
- Rozas, L. P. 1995. Hydroperiod and its influence on nekton use of the salt marsh: A pulsing ecosystem. *Estuaries* **18**: 579–590. doi:[10.2307/1352378](https://doi.org/10.2307/1352378)
- Saintilan, N., K. Rogers, C. Toms, E. D. Stein, and D. Jacobs. 2016. Intermittent estuaries: Linking hydro-geomorphic context to climate change resilience. *J. Coast. Res.* **75**: 133–137, doi:[10.2112/SI75-027.1](https://doi.org/10.2112/SI75-027.1), sp1
- Sanger, J. E., and E. Gorham. 1972. Stratigraphy of fossil pigments as a guide to the postglacial history of Kirchner Marsh, Minnesota. *Limnol. Oceanogr.* **17**: 840–854.
- Schuerch, M., and others. 2018. Future response of global coastal wetlands to sea-level rise. *Nature* **561**: 231–234. doi:[10.1038/s41586-018-0476-5](https://doi.org/10.1038/s41586-018-0476-5)
- Sievers, M., C. J. Brown, V. J. D. Tulloch, R. M. Pearson, J. A. Haig, M. P. Turschwell, and R. M. Connolly. 2019. The role of vegetated coastal wetlands for marine megafauna conservation. *Trends Ecol. Evol.* **34**: 807–817. doi:[10.1016/j.tree.2019.04.004](https://doi.org/10.1016/j.tree.2019.04.004)
- Sloss, C. R., B. G. Jones, C. V. Murray-Wallace, and C. E. McClennen. 2005. Holocene sea level fluctuations and the sedimentary evolution of a barrier estuary: Lake Illawarra, New South Wales, Australia. *J. Coast. Res.* **215**: 943–959. doi:[10.2112/03-0110.1](https://doi.org/10.2112/03-0110.1)
- Stephenson, D. B., V. Pavan, M. Collins, M. M. Junge, and R. Quadrelli. 2006. North Atlantic Oscillation response to transient greenhouse gas forcing and the impact on European winter climate: A CMIP2 multi-model assessment. *Climate Dynam.* **27**: 401–420. doi:[10.1007/s00382-006-0140-x](https://doi.org/10.1007/s00382-006-0140-x)
- Thorne, K. M., K. J. Buffington, S. F. Jones, and J. L. Largier. 2021. Wetlands in intermittently closed estuaries can

- build elevations to keep pace with sea-level rise. *Estuar. Coast. Shelf Sci.* **257**: 107386. doi:[10.1016/j.ecss.2021.107386](https://doi.org/10.1016/j.ecss.2021.107386)
- Uppala, S. M., and others. 2005. The ERA-40 re-analysis. *Q. J. Roy. Meteorol. Soc.* **131**: 2961–3012. doi:[10.1256/qj.04.176](https://doi.org/10.1256/qj.04.176)
- Vallentyne, J. R. 1955. Sedimentary chlorophyll determination as a paleobotanical method. *Can. J. Bot.* **33**: 304–313. doi:[10.1139/b55-026](https://doi.org/10.1139/b55-026)
- Viaroli, P., P. Lasserre, and P. Campostrini. 2007. Preface. *Hydrobiologia* **577**: 1–3. doi:[10.1007/s10750-006-0412-9](https://doi.org/10.1007/s10750-006-0412-9)
- Weis, P. 2016. Salt marsh accretion, p. 513–515. *In* M. J. Kennish [ed.], *Encyclopedia of estuaries*. Encyclopedia of earth sciences series. Springer.
- Wetzel, R. G. 2001. *Limnology: Lake and river ecosystems*, 3rd ed. Elsevier Academic Press
- Zhang, H.-M., J. J. Bates, and R. W. Reynolds. 2006. Assessment of composite global sampling: Sea surface wind speed. *Geophys. Res. Lett.* **33**: L17714. doi:[10.1029/2006GL027086](https://doi.org/10.1029/2006GL027086)

Acknowledgments

The authors acknowledged the Labgis system at the Rio de Janeiro State University, which together with local PCI Geomatica representation,

supported the development of the remote sensing methodology. Thanks are also due to the French Research Institute for Development (IRD) for the facilities, personal, and financial support in the sample analysis, and field excursion. We also appreciate Ibn Zohr for hospitality and support during the development of this thesis. Elemental and isotopic analyses were performed at the ALYSES platform, at the Institute of Research for Development - IRD (Bondy, France). Thanks are also due to the Czech University of Life Sciences Prague for the financial support regarding the publication of this manuscript. Finally, the authors thank for the valuable inputs of the anonymous reviewers. The authors would like to thank the financial support provided by the CAPES (Coordination for the Improvement of Higher Education Personnel) and CNPq (Brazilian National Council for Scientific and Technological Development) through the primary author's scholarship and project development (CNPQ 457400/2012-9), respectively. L.B. acknowledges the support from CHARISMA Project with the assistance of the Hassan II Academy of Sciences, Morocco.

Conflict of Interest

None declared.

Submitted 12 June 2021

Revised 10 September 2021

Accepted 14 November 2021

Deputy editor: Julia C. Mullarney